Seismic Fragility Assessment of Highway Bridge

S. Mahmoudi & L. Chouinard
Dept. of Civil Engineering, McGill University, QC, Canada

SUMMARY:
This paper addresses issues in the fragility analysis of bridges under seismic loads. The main objective of this paper is to generate fragility curves that account for all significant sources of uncertainties and to demonstrate the procedure for a case study.
In this paper, the effect of record-to-record variability in seismic inputs on the engineering demand parameters (EDP) is addressed by using the Incremental Dynamic Analysis (IDA) method. A 3-dimensional bridge model is developed and calibrated using ambient vibration test. The model is analyzed under a set of ground motion records (GMR) which are selected by using the conditional mean spectrum (CMS) based method. The variability in the strength of component materials, bearings and abutments are considered explicitly in the evaluation.
Component fragility curves are developed for each critical bridge components by utilizing probabilistic demand models (PDMs) obtained from regression analysis of component response. Finally, the system fragility curve of the bridge is generated by combining the component PDMs.

Keywords: System Fragility Curves, Component Fragility Curve, Incremental Dynamic Analysis, Conditional Mean Spectrum, Ambient Vibration Test

1. INTRODUCTION

Uncertainties involved in determining the demands from earthquakes and in evaluating the capacity of structures under cyclic loads are important inputs of probabilistic methods to quantitatively assess the reliability of structures. The seismic reliability of a structure can be evaluated by combining seismic hazards at the location of the structure and the fragility function of the structure. Fragility curves represent the state-of-the-art in seismic risk assessment (SRA) and are defined as the conditional probability that a structure will meet or exceed a certain level of damage for a given ground motion intensity.

The fragility analysis includes the following major steps;
i) The probabilistic representation of the bridge considering the uncertainty in its properties
ii) The selection of appropriate ground motions representing the effects of local site conditions and seismic inputs
iii) A 3-dimensional nonlinear analysis of the response of the structure, and
iv) The estimation of fragility curves from the response of the bridge model under the seismic loads considered.

This paper is organized into sections which follow the steps described above: Section 2 presents the finite element model of the bridge and its calibration based on ambient vibration tests; Section 3 discusses the selection of ground motion records based on site characteristics and structural response using the Conditional Mean Spectrum (CMS) method; Section 4 presents the Incremental Dynamic Analysis (IDA) of the bridge under the selected ground motion records and finally, Section 4 presents the component fragility curves for piers, bearings and abutments, and for the entire bridge

2. FINITE ELEMENT MODELING AND AMBIENT VIBRATION TEST

The bridge comprises three lanes, a bicycle path and a pedestrian walkway. The bridge is designated as a lifetime structure and needs to meet the highest standards in terms of reliability. The bridge consists of 5 spans with a total length of 232 meters. The superstructure consists of a concrete deck which is supported by 5 steel girders with varying depth. Except for the bearing at pier no.2, which is a low type fixed bearing, the other bearings at the piers and abutments are high steel bearings. The piers are located in the river bed and are supported by regular footings on hard rock.

The bridge is modeled with finite elements using SAP2000. A three dimensional view of the model is shown in Figure 1. The bridge deck and the girders are modeled with 4-node shell elements. The piers are modeled with nonlinear multi-layered shell elements. Cap beams are modeled with beam elements and the bearings and the abutments are modeled using Nllink elements which have six independent springs, one for each of six deformational degrees of freedom (SAP2000, 1996). Non-confined concrete material behaviour is assumed for the piers (Mander, 1988). The behaviour of the bearings is determined by finite element simulation in ABAQUS and the behaviour of the abutments is based on the model by Shamsabadi et al. (2007) for granular soils. The behaviour of abutments and bearing are shown in Figure 2.

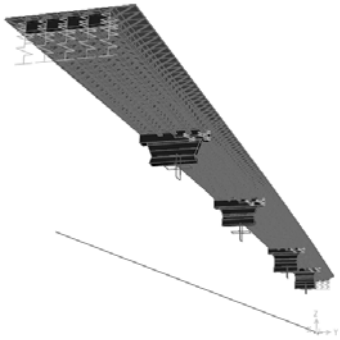

Figure 1. Three Dimensional view of Finite Element model of the bridge

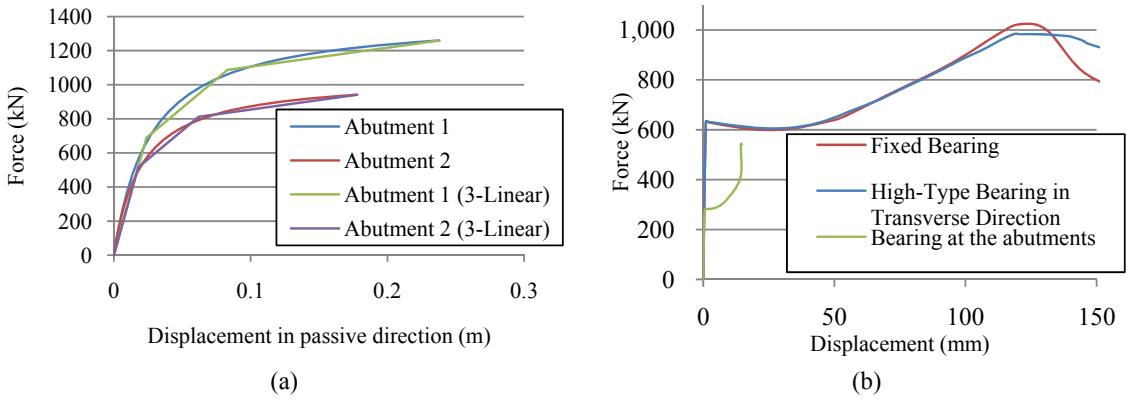

Figure 2. Force-Displacement relationship in a) Abutments b) Bearings

In contrast with the minor discrepancies between design and construction which are accounted for in fragility analysis, major deficiencies can have a significant influence on the vulnerability of a bridge. Ambient vibration testing has recently become a popular method for assessing the dynamic behaviour of full-scale structures. This test is especially suited to flexible systems. Ambient vibration surveys are non intrusive because no excitation equipment is needed since the natural or environmental excitations

are used which translates into minimal interference with the normal function of the structure. This test is used to estimate the natural frequencies of the structure which is representative of the dynamic behaviour of the structure when each component is minimally solicited (linear behaviour). This test has been used to calibrate the structural models and to identify major deficiencies in structural components, connections or supports. The first twenty natural frequencies of the structure are obtained using the EFDD (Enhanced Frequency Domain Decomposition) analysis. Table 1 compares the results obtained by the ambient vibration test and the finite element model.

Table 1. Comparison of natural frequencies obtained by the ambient vibration test and the finite element model

Mode number		1	2	3	4	5	6	7	8	9	10
Measured Frequency.	Cyc/sec	1.439	1.585	2.183	-	2.511	2.743	3.310	3.584	3.780	3.829
Model Frequency	Cyc/sec	1.428	1.603	1.979	2.409	2.588	2.699	3.192	3.534	3.813	3.890
Error	(%)	0.75	1.14	9.37	-	3.07	1.60	3.58	1.39	0.87	1.60

It is inferred from Table 1 that there are no significant deficiencies in the bridge structure. Also, the Finite Element Model is acceptable in the range of elastic behavior. However, it is noted that the fourth mode is not detected by the ambient vibration test, probably because this natural mode was not excited and detected during the test. In addition, it is noted that there is a rather higher error in the estimation of the third mode of the structure. The third mode corresponds to the longitudinal translational mode. This mode involves displacements in the expansion bearings. The higher error may be related to the nonlinear behavior of the bearings under environmental loads. Since some bearings may not be engaged by ambient noise, the structure appears to be stiffer in the ambient vibration tests compared to the finite element model.

3. SELECTION OF APPROPRIATE GROUND MOTION RECORDS

To select a set of ground motion records from an available database, one can match and compare the spectral acceleration of each ground motion with a target spectral acceleration. The Uniform Hazard Spectrum (UHS) has been traditionally used as a target spectrum to determine appropriate set of ground motions which are representative of the site seismicity. However, UHS is not the best target spectrum for this purpose because UHS conservatively considers the Spectral Accelerations (Sa) with low probability of occurrence at all periods. However, it is unlikely to find a single ground motion record with Sa higher than median over a wide range of periods.

Baker and Cornell (2006) introduced the “Conditional Mean Spectrum” (CMS) as a suitable alternative for the target spectrum. The main purpose of introducing CMS is to provide the expected response spectrum, conditioned on occurrence of a target spectral acceleration value at the period of interest (e.g. at the first natural period of the structure). By determining the Sa at the first period of the structure from UHS and developing CMS to choose appropriate ground motion records, the characteristics of both structure and site seismicity is taken into account.

In this paper, CMS is developed based on the seismicity of Montreal and the natural frequency of the bridge. For this purpose, the procedure suggested by Baker (2011) is applied. First, the mean value of magnitude (M) and distance (R) of earthquakes is determined by deaggregation of the seismic hazard for Montreal for a probability of exceedance of 2% in 50 years. According to Adams et al. (2004) the values of M=6.8 and R=57 km are the representative values for Montreal. Then, a target value for Sa at the first period of the bridge is determined. It is shown in section 2 that the first period of the bridge is 0.7 second. The target Sa corresponding to this period is determined using the UHS of Montreal (Geological Survey of Canada (GSC), 2005). Soil characteristics at the location of the bridge are determined based on the seismic microzonation map developed by Chouinard et al. (2011).
The next step is to estimate the mean and standard deviation of the natural logarithm of the Sa at

various periods. For this purpose, the Ground Motion Prediction Equations developed by Atkinson and Boore (2006, 2008) are used. Finally, CMS is implemented by using equation 1. (Baker, 2011)

$$\mu_{lnS_a(T_i)|lnS_a(T_n)} = \mu_{lnS_a}(\bar{M}, \bar{R}, T_i) + \rho(T_i, T^*)\bar{\varepsilon}(T^*)\sigma_{lnS_a}(T_i) \quad (1)$$

where $\mu_{lnS_a}(\bar{M}, \bar{R}, T_i)$ and $\sigma_{lnS_a}(T_i)$ are the mean and standard deviation of the natural logarithm of Sa at the first period of the structure. $\bar{M}$, $\bar{R}$, and $\bar{\boldsymbol{\varepsilon}}(T_n)$ are the mean magnitude, mean distance and mean value of epsilon at the considered period T_n, respectively (epsilon is the number of logarithmic standard deviations of a target ground motion from a median ground motion). $\rho(T_i, T_n)$is the inter-period correlation of spectral accelerations at vibration periods T_i and T^*.

The predicted median spectrum, UHS and CMS are presented in figure 3. It is noted that CMS and UHS have the same Sa at the first period of the structure but the CMS has lower Sa at the other periods.

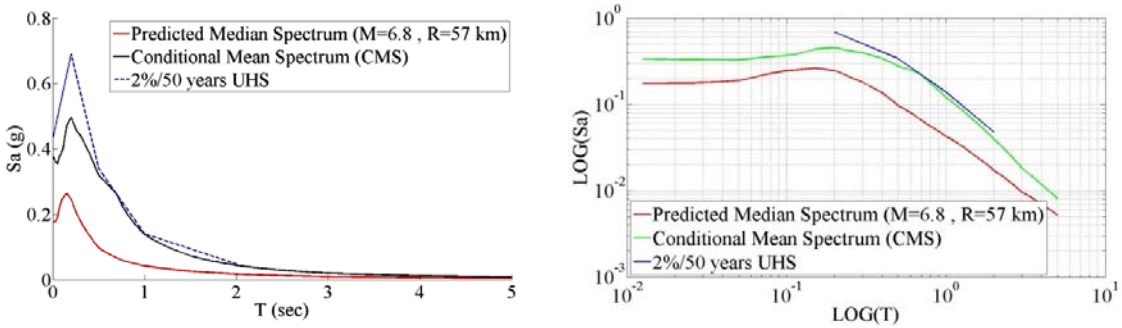

(a) (b)

Figure 3. (a) CMS versus prediction Median Spectrum and UHS
(b) CMS versus prediction Median Spectrum and UHS in log-log space

Once the CMS is developed, it can be used as the target spectrum to select the ground motion set for dynamic analysis. For this purpose, a period range from 0.2 to 2 times the first period of the structure is considered to match the CMS. All the ground motion records of the available database are scaled so that their Sa at the first period of the structure ($Sa(T_1)$) matches the target spectral acceleration from the CMS. Then the Sum of Squared Errors (SSE) is calculated for each ground motion record and the records with the lowest SSE are selected as representative earthquakes for dynamic analysis.

In this paper, the PEER-NGA database which offers 3541 ground motion records from 175 earthquakes is used. Figure 4 represents the CMS and the Sa of the selected earthquake records. The first ten selected ground motion records are presented in table 2.

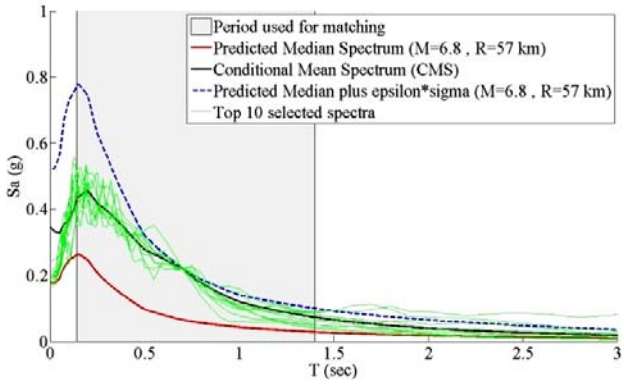

Figure 4. CMS and Sa of the top ten selected ground motion records

Table 2. Top ten selected ground motion records for dynamic analysis

	Earthquake	year	Station	Magnitude	Distance (km)
1	'Chi-Chi, Taiwan-06'	1999	'CHY076'	6.3	84.34
2	'Lazio-Abruzzo, Italy'	1984	'Pontecorvo'	5.8	29.72
3	'Chi-Chi, Taiwan-06'	1999	'TCU075'	6.3	36.04
4	'Chi-Chi, Taiwan-02'	1999	'CHY112'	5.9	88.21
5	'Imperial Valley-07'	1979	'El Centro Array #3'	5.01	15.28
6	'Chi-Chi, Taiwan-02'	1999	'CHY027'	5.9	80.45
7	'Chi-Chi, Taiwan-02'	1999	'CHY039'	5.9	82.34
8	'Imperial Valley-07'	1979	'Calexico Fire Station'	5.01	11.85
9	'Tabas, Iran'	1978	'Ferdows'	7.35	117.66
10	'Coalinga-05'	1983	'Pleasant Valley P.P. - yard'	5.77	16.17

4. INCREMENTAL DYNAMIC ANALYSIS (IDA)

The variability in seismic inputs is a significant source of uncertainty in the seismic evaluation of structures. The IDA technique (Vamvatsikos and Cornell, 2002) addresses the record-to-record variability by using a set of scaled input ground motions to evaluate the response of a structure. By performing non-linear dynamic analysis under several scaling factors, for each ground motion record, the relationship of the Intensity Measure (IM) and the Engineering Demand Parameter (EDP) is obtained. The selection of the proper ground motion records, EDP and IM for the structure should be done carefully since they can all affect the results.

In this paper, displacements in piers, bearings and abutments are considered as EDPs and the spectral acceleration (Sa) at the first natural period of the structure is selected as IM. In addition, ground motions are assumed to occur in the transverse direction and the IM of the records is scaled up from 0.02g to 1g.

It has been suggested by Cornell et al. (2002) that the estimate of the median demand ($\widehat{\mathrm{EDP}}$) can be represented by a power model as shown in equation 2.

$$\widehat{\mathrm{EDP}} = \mathrm{a}.\,\mathrm{IM}^{\mathrm{b}} \tag{2}$$

where IM is the seismic intensity measure and both a and b are regression coefficients. The variation about the median ($\beta_{EDP|IM}$) is assumed to be lognormal. Therefore, in the following transformed space, this variation should be normal.

$$Ln\left(\widehat{EDP}\right) = Ln(a) + b.Ln(IM) \tag{3}$$

Figure 5 represents the relation between $Ln\left(\widehat{EDP}\right)$ and $Ln(IM)$ obtained from IDA and the regression model for bearing at the abutments, bearings on piers and piers.

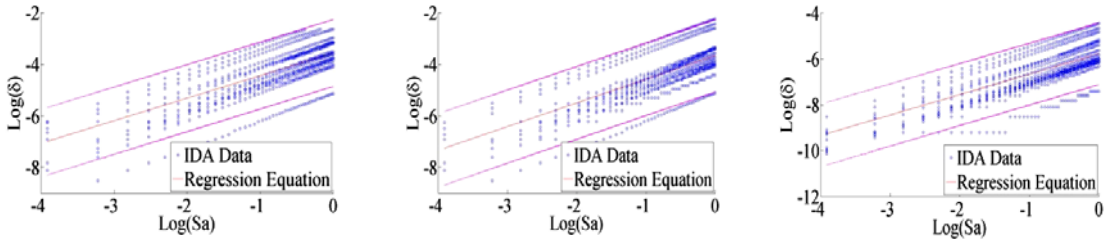

Figure 5. IDA results and regression model for (a) Bearing at the Abutment 1 (b) Bearing on the 1 (c) Pier 3

5. FRAGILITY CURVES

A fragility curve is the conditional probability that the structure or structural component sustains the specified damage-level or limit state for a given ground motion intensity. Assuming lognormal distributions for the probabilistic seismic demand model and the structural capacity, fragility curves are determined from equation 4.

$$P\left[\frac{D}{C} \geq 1 \mid IM\right] = \Phi\left(\frac{Ln(E\widehat{D}P/S_c)}{\sqrt{{\beta_{D|IM}}^2 + {\beta_c}^2}}\right) \tag{4}$$

in which $E\widehat{D}P$ is the median of demand at the selected IM, S_c is the median of the selected limit state, $\beta_{D|IM}$ is the logarithmic standard deviations of demands and β_c is the logarithmic standard deviation of the limit state (capacity).

Fragility curves can be developed for structural components as well as for the structure as a whole system. By considering variability in seismic inputs, structure response, and material capacity into account, component fragility curves are useful tools to identify weak parts of the structure and to guide for the efficient allocation of funds to strengthen or retrofit an existing structure while system fragility curves are useful in seismic risk assessment of the structure.

5.1. Component Fragility Curves

Component fragility curves are developed for the abutments, bearings and piers for two limit states of slight damage and dynamic instability (collapse). The limit states are defined based on the behaviour of each component and are shown in Table 3. It is noted that the piers have a fairly brittle behaviour in transverse direction and the slight damage limit state is assumed to be equal to 0.9 times the collapse limit state.

Table 3. Quantitative Limit states for structural components

Limit State	Bearing at the Abutments (mm)	Bearing at the piers (mm)	Pier 3 (mm)
Slight damage	0.81	1.4	7.2
Collapse	14.2	124	8

To develop component fragility curves, $E\widehat{D}P$ is estimated at various IMs using equation 3 and the fragility curves are assumed to have lognormal distribution as represented in equation 4. Component fragility curves for selected elements are shown in figure 6.

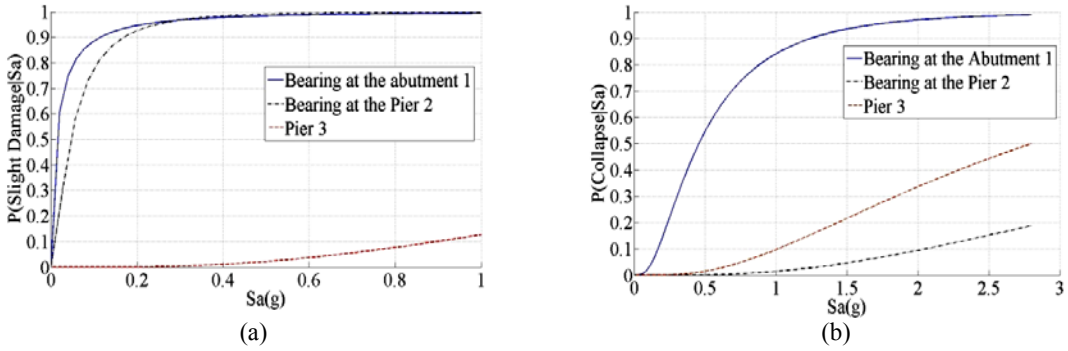

Figure 6. Component Fragility curves for (a) Slight damage Limit State (b) Collapse Limit State

5.2. System Fragility Curves

To develop the system fragility curve, the IMs in which the ground motion records forces the structure to collapse are detected from IDA results. It is noted that during different ground motions, the collapse may occur in different components. A Bernoulli random variable is used to show whether or not the bridge sustains collapse, and Logistic model is used to develop the system fragility curve. Moreover, the distribution parameters are determined through a logistic regression analysis. For this purpose, the inverse cumulative distribution function of the logistic distribution as presented in equation 5 is applied.

$$F^{-1}(p;\mu,s) = \mu + s.\ln\left(\frac{p}{1-p}\right) \tag{5}$$

In which F^{-1} represents the vector of spectral accelerations in which collapse occurred in the structure, p is the vector representing the probability of collapse at corresponding spectral accelerations and μ and s are the mean and standard deviation of the logistic distribution which are evaluated through the regression. It is noted that for each Sa, p is estimated by counting the number of earthquakes which cause collapse in structure with lower spectral acceleration. The system fragility of the bridge for collapse limit state is presented in figure 7.

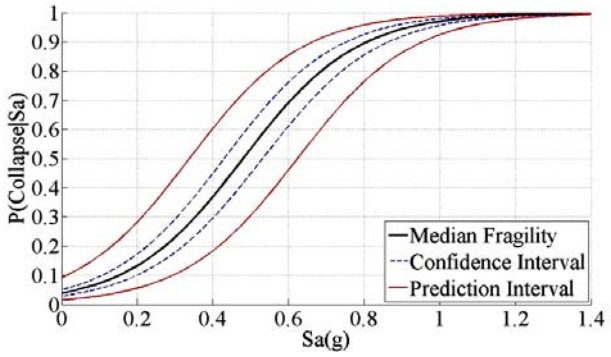

Figure 7. System fragility curve for collapse limit state

6. CONCLUSION

In this paper, fragility curves are developed for a bridge which is located in Montreal. Three critical components are selected to represent the component fragility curves: Bearing at the abutment 1, Bearing at the pier 2 and pier 3. Despite the brittle behaviour of the piers, they are not the critical elements for either of the selected limit states because they are isolated by the bearings. The bearings

at the piers are designed to have high ductility. It is inferred from figure 6 that the probability of collapse of these bearings is lower than other components. However, their flexible behaviour causes these bearings to reach their slight damage limit state by earthquakes with very low spectral accelerations.

Figure 6 (a) demonstrates that the bearings at the abutments and the bearings at the piers reach their slight damage limits almost at the same point. However, the bearings at the piers withstand significant displacements at the slight damage limit state. Hence, they impose higher displacement demands to the structure and can cause other modes of failure such as fatigue. In other words, the flexible behaviour of the bearings at the piers can cause high displacements and failures in adjacent components even under regular usage of the bridge.

Comparing figures 6(b) and 7, it is inferred that the bearings at the abutments have the highest contribution in system fragility of the bridge. These bearings have very low ductility and cause unseating at the abutments. The median Sa at which unseating occurs is equal to 0.43g which is lower than the requirements of standards for a lifetime bridge.

REFERENCES

Adams J, Halchuk S. (2003). Fourth generation seismic hazard maps of Canada: Values for over 650 Canadian localities intended for the 2005 National Building Code of Canada. *Geological Survey of Canada Open File 2003*; **4459**: 1-155.

Adams, J., Halchuk, S. (2004). Fourth-Generation Seismic Hazard Maps for the 2005 National Building Code of Canada. *13th World Conference on Earthquake Engineering.* Paper 2502. Vancouver, B.C., Canada

Atkinson, G. M. and D. M. Boore (2006). Earthquake ground-motion prediction equations for eastern North America, *Bull. Seism. Soc. Am.* **96**, 2181--2205.

Baker, J.W. (2011). Conditional Mean Spectrum: Tool for ground motion selection, *Journal of Structural Engineering*, **137(3)**, 322-331.

Baker, J. W., and Cornell, C. A. (2006). Correlation of response spectral values for multicomponent ground motions. *Bulletin of the Seismological Society of America*, **96(1)**, 215-227.

Boore, D. M. and G. M. Atkinson (2008). Ground-motion prediction equations for the average horizontal component of PGA, PGV, and 5%-damped PSA at spectral periods between 0.01 s and 10.0 s, *Earthquake Spectra* **24**, 99-138.

Chouinard, L. And Rosst, P. (2011). Microzonation of Montreal, Variability in Soil Classification. *4th IASPEI/IAEE International Symposium.* University of California Santa Barbara

Cornell, A. C., Jalayer, F., and Hamburger, R. O. (2002). Probabilistic Basis for 2000 SAC Federal Emergency Management Agency Steel Moment Frame Guidelines. *Journal of Structural Engineering*, **128(4)**, 526–532.

Mander, J.B., Priestley, M.J.N., and Park, R. (1988). Theoretical stress-strain model of confined concrete. *J. Struct. Eng.*,**114(8)**, 1804-1826.

SAP2000, (1996). Integrated Finite Element Analysis and Design of Structures: Analysis Reference. *Computers and Structures, Inc.*, Berkeley, CA.

Shamsabadi, A., Rollins, K. M., and Kapuskar, M. (2007). Nonlinear soil-abutment-bridge structure interaction for seismic performance-based design. *Journal of Geotechnical and Geoenvironmental Engineering*, **133(6)**, 707-720.

Vamvatsikos, D. and Cornell, A. C. (2002). Incremental Dynamic Analysis. *Earthquake Engineering & Structural Dynamics*, **31**, 491–514.